Research Square

Preprints are preliminary reports that have not undergone peer review.
They should not be considered conclusive, used to inform clinical practice,
or referenced by the media as validated information.

Constrained Dynamic Output Feedback Tracking via Internal Models and Polyhedral Invariant Sets

Geovana França dos Santos

geovana.francadossantos@mail.concordia.ca

Concordia University

Eugênio B. Castelan

Universidade Federal de Santa Catarina

Walter Lucia

Concordia University

Jackson G. Ernesto

Universidade Federal de Santa Catarina

Research Article

Keywords: Constrained Control, Dynamic Output Feedback, Internal Model Principle, Robust Positive Invariance, Bilinear Programming

Posted Date: October 6th, 2026

DOI: https://doi.org/10.21203/rs.3.rs-11063676/v1

License: This work is licensed under a Creative Commons Attribution 4.0 International License.
Read Full License

Additional Declarations: No competing interests reported.

Constrained Dynamic Output Feedback Tracking via Internal Models and Polyhedral Invariant Sets

Geovana França dos Santos[1,2*], Eugênio B. Castelan[2*], Walter Lucia[1] and Jackson G. Ernesto[2]

[1*]Department of Cybersecurity and Intelligent Systems Engineering (CISE), Concordia University, Montreal, QC, H3G-1M8, Canada.
[2]Graduate Program in Automation and Systems Engineering, Federal University of Santa Catarina (UFSC), Florianópolis, SC, 88040-900, Brazil.

*Corresponding author(s). E-mail(s): geovana.francadossantos@mail.concordia.ca; eugenio.castelan@ufsc.br;
Contributing authors: walter.lucia@concordia.ca; jackson.ernesto@posgrad.ufsc.br;

Abstract

Guaranteeing reference tracking under actuator and state limitations remains a central challenge in constrained control design, particularly when the class of exogenous signals to be tracked extends beyond simple step inputs. This work develops a synthesis framework for dynamic output feedback controllers that achieve asymptotic, offset-free tracking of a broad family of reference signals, encompassing steps, ramps, sinusoids, and parabolic profiles, under simultaneous state and input polyhedral constraints. The controller architecture combines a generalized internal model, feedforward compensation, and a dynamic output feedback compensator, and its gains are obtained through a single offline bilinear optimization problem built on robust positive invariance theory and the Extended Farkas' Lemma. Unlike approaches that fix the admissible operating set a priori, the proposed method simultaneously determines, as part of the same optimization, the sets of initial conditions for which constraint admissibility and stability are certified. The effectiveness and robustness of the resulting control synthesis are demonstrated through numerical simulations.

Keywords: Constrained Control, Dynamic Output Feedback, Internal Model Principle, Robust Positive Invariance, Bilinear Programming

1 Introduction

Reference tracking is a fundamental objective in control systems and is required in a wide range of engineering applications, including process control, robotics, aerospace systems, autonomous vehicles, and power electronics. In these applications, the controller must follow time-varying reference trajectories while satisfying physical limitations imposed by actuator saturation, safety requirements, and operational limits.

Furthermore, many practical systems do not provide full-state measurements due to sensor limitations, cost, or partial observability, making output feedback controllers a necessity rather than a design choice. Consequently, developing

output-feedback tracking controllers that simultaneously guarantee asymptotic tracking, closed-loop stability, and constraint satisfaction remains a fundamental challenge in modern control.

For unconstrained linear systems, the Internal Model Principle (IMP) (Chen 2014; Francis and Wonham 1976) provides the foundational framework for achieving asymptotic tracking and disturbance rejection. By embedding a dynamic model of the exogenous signals directly within the feedback loop, the IMP guarantees zero steady-state tracking error for persistent reference signals generated by known dynamics. However, when constrained setups are of interest, the IMP must be carefully applied because its validity is restricted to the region where the constraints are inactive. Therefore, when state and input constraints are present, tracking becomes significantly more challenging.

Several approaches have been investigated to address constrained tracking problems, each with its own advantages and limitations. Model Predictive Control (MPC) provides a systematic framework for explicitly enforcing constraints while optimizing closed-loop performance (Limon et al. 2005; Ferramosca et al. 2011; Di Cairano and Borrelli 2015), but its online computational burden limits its applicability in fast or embedded implementations. Reference and command governors reduce this burden by modifying the reference signal online while preserving the existing controller structure (Garone et al. 2017; Gilbert and Ong 2011; Casavola et al. 2000); however, since the tracking controller itself is not redesigned, this reference modification can introduce performance limitations. Linear Matrix Inequality (LMI)-based approaches provide systematic synthesis with formal stability guarantees (Flores et al. 2011; Figueiredo et al. 2020; Flores et al. 2009), although they typically rely on conservative ellipsoidal invariant sets and symmetric saturation assumptions. Across these approaches, each design is generally tailored to one particular reference signal, commonly step (Limon et al. 2005; Ferramosca et al. 2011; Garone et al. 2017) or periodic signals (Flores et al. 2011, 2009), with the admissible operating region fixed a priori rather than synthesized jointly with the controller.

This paper proposes a constrained tracking control synthesis for continuous-time linear systems subject to polyhedral state and input constraints. The framework combines a generalized internal model, a Dynamic Output Feedback (DOF) controller, and a reference feedforward compensator to enable asymptotic, offset-free tracking of diverse persistent references, including step, ramp, sinusoidal, and parabolic signals. A key feature of this approach is the joint computation of the controller gains, the invariant set, and the internal-model limits, avoiding the conservatism of sequential design or predefined parameters. By combining Robust Positive Invariance (RPI) theory (Blanchini and Miani 2015) with the Extended Farkas' Lemma (Hennet 1995), this synthesis is cast as a single offline bilinear optimization program that characterizes the domain of attraction while guaranteeing constraint satisfaction and stability. Finally, this generalized framework encompasses our earlier static output-feedback and single-reference formulations (Santos et al. 2023, 2024) as particular cases.

The remainder of this paper is organized as follows. Section 2 formulates the constrained tracking problem. Section 3 presents the proposed RPI-based synthesis conditions and optimization framework. Section 4 illustrates the effectiveness of the proposed method through numerical simulations, and Section 5 concludes the paper.

Notation: $\mathbb{R}$ and $\mathbb{R}_{>0}$ denote the sets of real and positive real numbers, respectively. $\mathbb{R}^n$ denotes the n-dimensional Euclidean space, and $\mathbb{R}^{n\times m}$ denotes the set of $n \times m$ real matrices. The identity matrix of order n is denoted by I_n, and $0_{n\times m}$ is an $n \times m$ zero matrix. The vector of ones of dimension n is denoted by $\mathbf{1}_n$. For vectors $a, b \in \mathbb{R}^n$, $a \leq b$ indicates element-wise inequality, and a matrix M is non-negative ($M \geq 0$) if $M_{ij} \geq 0$ for all i, j. A square matrix H is called a Metzler matrix if $H_{ij} \geq 0$ for all $i \neq j$. The spectrum of a matrix A is denoted by $\sigma(A)$, while $\text{rank}(A)$ and $\text{trace}(A)$ denote its rank and trace. The Minkowski set addition is denoted by $\oplus$.

2 Constrained Control Problem

Consider a linear time-invariant continuous-time (LTIC) system governed by

$$\dot{x}(t) = Ax(t) + Bu(t), \tag{1a}$$
$$y(t) = Cx(t), \tag{1b}$$

where $x(t) \in \mathbb{R}^{n_x}$ is the state vector, $u(t) \in \mathbb{R}^{n_u}$ is the control input, and $y(t) \in \mathbb{R}^{n_y}$ is the output vector. The system state and control input are subject to polyhedral constraint sets defined by

$$\mathcal{X} = \{x(t) \in \mathbb{R}^{n_x} : Xx(t) \leq \mathbf{1}_{l_x}\}, \tag{2}$$
$$\mathcal{U} = \{u(t) \in \mathbb{R}^{n_u} : Uu(t) \leq \mathbf{1}_{l_u}\}, \tag{3}$$

with $X \in \mathbb{R}^{l_x \times n_x}$ and $U \in \mathbb{R}^{l_u \times n_u}$.

Remark 1 To simplify the notation, we omit the explicit dependence of x, y, and u on t hereafter.

2.1 Reference Signal and Internal Model Principle

The tracking error is defined as

$$e = r - y, \tag{4}$$

where $r \in \mathbb{R}^{n_y}$ is an exogenous reference signal to be tracked. Specifically, each reference channel is governed by a homogeneous differential equation of order $n_{x_I} \in \{1, 2, 3\}$:

$$r^{(n_{x_I})} + \alpha_{n_{x_I}-1} r^{(n_{x_I}-1)} + \cdots + \alpha_1 \dot{r} + \alpha_0 r = 0. \tag{5}$$

Table 1 summarizes the four canonical reference signals considered in this work, along with their corresponding generator dynamics.

According to the Internal Model Principle (IMP) (Francis and Wonham 1976; Chen 2014), to achieve asymptotic zero steady-state tracking error under persistent exogenous reference modes, a replica of the reference generator dynamics must be embedded within the feedback loop. To this end, the internal model dynamics driven by the tracking error e are structured as:

$$\begin{aligned} \dot{x}_I &= A_I x_I + B_I e, \\ u_I &= C_I x_I + D_I e, \end{aligned} \tag{6}$$

Table 1 Reference Signal Properties

Signal	Trajectory	Differential Eq.	n_{x_I}
Step	a	$\dot{r} = 0$	1
Ramp	at	$\ddot{r} = 0$	2
Sinusoid	$a\sin(\omega t)$	$\ddot{r} + \omega^2 r = 0$	2
Parabola	at^2	$\dddot{r} = 0$	3

Table 2 Internal Model Matrices (A_I, B_I) for $n_y = 1$

Signal	Step	Ramp	Sinusoid	Parabola
A_I	$\begin{bmatrix} 0 \end{bmatrix}$	$\begin{bmatrix} 0 & 0 \\ 1 & 0 \end{bmatrix}$	$\begin{bmatrix} 0 & -\omega^2 \\ 1 & 0 \end{bmatrix}$	$\begin{bmatrix} 0 & 0 & 0 \\ 1 & 0 & 0 \\ 0 & 1 & 0 \end{bmatrix}$
B_I	$\begin{bmatrix} 1 \end{bmatrix}$	$\begin{bmatrix} 1 & 0 \end{bmatrix}^\top$	$\begin{bmatrix} 1 & 0 \end{bmatrix}^\top$	$\begin{bmatrix} 1 & 0 & 0 \end{bmatrix}^\top$

where $x_I \in \mathbb{R}^{n_{x_I}}$ represents the internal model state vector, while $C_I \in \mathbb{R}^{n_u \times n_{x_I}}$ and $D_I \in \mathbb{R}^{n_u \times n_y}$ are parameter matrices to be synthesized.

The structural pair (A_I, B_I) represents the controllable canonical realization of the generator dynamics (5), where $x_I = \begin{bmatrix} x_{I_1} & \cdots & x_{I_{n_{x_I}}} \end{bmatrix}^\top$ stores the integrator states driven by the tracking error. Explicitly, the state-space realizations for each canonical reference signal are defined by the structural matrices in Table 2.

Remark 2 For polynomial reference profiles (step, ramp, and parabola), A_I forms a pure chain of integrators ($\alpha_i = 0$), recovering the classical state-space integral error framework (Franklin et al. 2010). For sinusoidal signals, the internal cross-coupling term $-\omega^2$ sustains harmonic oscillations within the internal model state space.

For multi-output plants ($n_y > 1$), independent internal models of the same structural type are embedded for each output channel to achieve steady-state tracking. Consequently, each channel $p \in \{1, \ldots, n_y\}$ shares the state dimension n_{x_I}, while permitting channel-specific parameters (e.g., distinct frequencies ω_p in sinusoidal references).

The global internal model state vector expands to $\mathbf{x}_I = [(x_I^{(1)})^\top, \ldots, (x_I^{(n_y)})^\top]^\top \in \mathbb{R}^{n_y n_{x_I}}$, where $x_I^{(p)} \in \mathbb{R}^{n_{x_I}}$ denotes the internal model state vector of channel p. The corresponding global system matrices

take the block-diagonal form:

$$\mathbf{A}_I = \mathrm{diag}(A_{I,1}, \ldots, A_{I,n_y}) \in \mathbb{R}^{(n_y n_{x_I}) \times (n_y n_{x_I})},$$
$$\mathbf{B}_I = \mathrm{diag}(B_{I,1}, \ldots, B_{I,n_y}) \in \mathbb{R}^{(n_y n_{x_I}) \times n_y},$$

where $(A_{I,p}, B_{I,p})$ is the canonical pair for channel p.

To ensure the plant can track the reference signal without blocking its essential frequencies, the plant matrix must not have transmission zeros at the characteristic frequencies of r.

Assumption 1 The pair (A, B) is controllable and (A, C) is observable. Furthermore, the plant (A, B, C) has no transmission zeros at the characteristic roots $\lambda \in \mathbb{C}$ of the reference generator differential equation (5) (Chen 2014). Formally, the system matrix satisfies:

$$\mathrm{rank} \begin{bmatrix} A - \lambda I_{n_x} & B \\ C & 0 \end{bmatrix} = n_x + n_y. \tag{7}$$

Depending on the reference signals in Table 1, condition (7) is evaluated across two distinct cases:

- *Zero-frequency modes ($\lambda = 0$):* For step, ramp, and parabolic references, this ensures the absence of transmission zeros at the origin, maintaining internal model controllability for offset-free polynomial tracking.
- *Resonant-frequency modes ($\lambda = \pm j\omega$):* For sinusoidal references, this ensures the plant does not block the reference frequency ω, allowing harmonic internal model modes to be sustained without plant attenuation.

2.2 Controller Architecture and Closed-Loop Dynamics

To provide dynamic stabilization and reference tracking, the internal model (6) is integrated with a dynamic output-feedback controller:

$$\begin{aligned} \dot{x}_c &= A_c x_c + B_c y, \\ u_c &= C_c x_c + D_c y, \end{aligned} \tag{8}$$

where $x_c \in \mathbb{R}^{n_c}$ is the dynamic controller state vector, $A_c \in \mathbb{R}^{n_c \times n_c}$, $B_c \in \mathbb{R}^{n_c \times n_y}$, $C_c \in \mathbb{R}^{n_u \times n_c}$, and $D_c \in \mathbb{R}^{n_u \times n_y}$.

Combining the dynamic controller output u_c, the internal model output u_I, and a reference feedforward channel $u_r = D_r r$, with $D_r \in \mathbb{R}^{n_u \times n_y}$, the control input is structured as $u = u_c + u_I + u_r$. Substituting (6), (8), and $e = r - Cx$ yields

$$u = (D_c - D_I)Cx + C_c x_c + C_I x_I + (D_I + D_r) r. \tag{9}$$

In practical applications, unconstrained integration of the tracking error e can lead to severe integrator windup when actuators have finite capacity (Tarbouriech et al. 2011; Åström et al. 2006). To avoid these effects, the internal model states are constrained to the polyhedral set:

$$\mathcal{X}_I = \left\{ x_I \in \mathbb{R}^{n_{x_I}} : X_I x_I \leq \mathbf{1}_{2n_{x_I}} \right\}, \tag{10}$$

where $X_I = \begin{bmatrix} X_{I,1} \\ -X_{I,2} \end{bmatrix} \in \mathbb{R}^{2n_{x_I} \times n_{x_I}}$ and

$$X_{I,j} = \mathrm{diag}(\xi_{j,1}, \ldots, \xi_{j,n_{x_I}}) > 0, \quad j \in \{1, 2\}.$$

The resulting set $\mathcal{X}_I$ restricts each state component to the asymmetric interval

$$-\xi_{2,k}^{-1} \leq x_{I,k} \leq \xi_{1,k}^{-1}, \quad k = 1, \ldots, n_{x_I}.$$

Furthermore, the exogenous reference signal r is assumed to belong to the set:

$$\mathcal{R} = \{ r \in \mathbb{R}^{n_y} : Rr \leq \rho \}, \tag{11}$$

with $R = \begin{bmatrix} I_{n_y} \\ -I_{n_y} \end{bmatrix} \in \mathbb{R}^{2n_y \times n_y}$ and $\rho = \begin{bmatrix} \rho_1 \\ \rho_2 \end{bmatrix} \geq 0 \in \mathbb{R}^{2n_y}$.

Over any operational horizon $t \in [0, T]$ with $T > 0$, the vector ρ provides clear physical bounds on the reference signals:

- *Step $r = a$*: ρ bounds the steady-state magnitude, i.e., $|a| \leq \rho$.
- *Ramp $r = at$*: ρ bounds the slope $|a| \leq \rho/T$.
- *Sinusoidal $r = a\sin(\omega t)$*: ρ bounds the peak amplitude $|a| \leq \rho$, while the frequency parameter ω enters explicitly via the internal model matrix A_I.
- *Parabolic $r = at^2$*: ρ bounds the acceleration scaling $|a| \leq \rho/T^2$.

While the IMP ensures asymptotic tracking, unbounded references require a finite horizon under physical constraints; here, T is chosen sufficiently large to ensure that the tracking error becomes negligible for the ramp and parabolic signals.

The problem can be formulated as follows:

Problem 1 *Consider the constrained LTIC plant (1)–(3), subject to the reference set (11), internal model state bounds (10), and the control architecture that results in (9). Under Assumption 1, design the controller gain tuple $(A_c, B_c, C_c, D_c, C_I, D_I, D_r)$, the allowable reference bound vector ρ in (11) (if not preassigned), and an admissible domain of attraction $\mathcal{L} \subset \mathbb{R}^{n_\xi}$ such that for every initial composite state $\xi(0) \in \mathcal{L}$ and valid reference trajectory $r \in \mathcal{R}$:*

1. *Asymptotic reference tracking is guaranteed, i.e., $\lim_{t\to\infty} e = 0$;*
2. *State, input, and internal model constraints (2), (3), and (10) are satisfied for all $t \geq 0$.*

3 Proposed Solution

To solve Problem 1, we leverage polyhedral RPI and algebraic set-containment conditions based on the Extended Farkas' Lemma (reviewed in Appendix A). By characterizing the augmented closed-loop dynamics under the dynamic output-feedback law (9), the synthesis of the controller gains, internal model bounds, and the certified RPI domain $\mathcal{L}$ is formulated as a single offline bilinear program via Theorem 1.

To this end, let the augmented state vector be defined as

$$\xi = \begin{bmatrix} x \\ x_c \\ x_I \end{bmatrix} \in \mathbb{R}^{n_\xi}, \text{ where } n_\xi = n_x + n_c + n_{x_I},$$

and substituting the plant output $y = Cx$ into the dynamic compensator (8), the tracking error $e = r - Cx$ into the internal model (6), and the resulting control law (9) into the plant dynamics (1), the closed-loop system is described by

$$\dot{\xi} = A_{cl}\xi + B_{cl}r, \tag{12}$$

with

$$A_{cl} = \begin{bmatrix} A + B(D_c - D_I)C & BC_c & BC_I \\ B_cC & A_c & 0_{n_c \times n_{x_I}} \\ -B_IC & 0_{n_{x_I} \times n_c} & A_I \end{bmatrix},$$
$$B_{cl} = \begin{bmatrix} B(D_I + D_r) \\ 0_{n_c \times n_y} \\ B_I \end{bmatrix}.$$

Under the control law (9), the control input constraint $u \in \mathcal{U}$ expressed in (3) transforms into an augmented constraint on the closed-loop state ξ and exogenous input r:

$$\mathcal{U}_{cl} = \{(\xi, r) : UK_\xi\xi + UK_r r \leq \mathbf{1}_{l_u}\}, \tag{13}$$

where the composite feedback gain $K_\xi \in \mathbb{R}^{n_u \times n_\xi}$ and feedforward gain $K_r \in \mathbb{R}^{n_u \times n_y}$ are partitioned as

$$K_\xi = \begin{bmatrix}(D_c - D_I)C & C_c & C_I\end{bmatrix}, \quad K_r = D_I + D_r.$$

Similarly, aggregating plant state constraints (2) and internal model state bounds (10) yields the composite state polyhedral set

$$\mathcal{X}_{cl} = \left\{\xi \in \mathbb{R}^{n_\xi} : X_{cl}\xi \leq \mathbf{1}_{l_x + 2n_{x_I}}\right\}, \tag{14}$$

where the global state constraint matrix $X_{cl} \in \mathbb{R}^{(l_x + 2n_{x_I}) \times n_\xi}$ is structured as

$$X_{cl} = \begin{bmatrix} X & 0_{l_x \times n_c} & 0_{l_x \times n_{x_I}} \\ 0_{2n_{x_I} \times n_x} & 0_{2n_{x_I} \times n_c} & X_I \end{bmatrix}.$$

Remark 3 The closed-loop framework (12) unifies and generalizes our prior static output-feedback formulations. Specifically, by considering a static output-feedback controller in the internal path, i.e., $u_c = D_c y$ (setting $n_c = 0$), and single IMP controllers, with $D_I = 0$, the control law (9) and the closed-loop dynamics (12) simplify to the static baseline:

$$u = \begin{bmatrix}D_cC & C_I\end{bmatrix}\begin{bmatrix} x \\ \mathbf{x}_I \end{bmatrix} + D_r r,$$

$$\begin{bmatrix} \dot{x} \\ \dot{\mathbf{x}}_I \end{bmatrix} = \begin{bmatrix} A + BD_cC & BC_I \\ -\mathbf{B}_IC & \mathbf{A}_I \end{bmatrix}\begin{bmatrix} x \\ \mathbf{x}_I \end{bmatrix} + \begin{bmatrix} BD_r \\ \mathbf{B}_I \end{bmatrix} r,$$

with proportional gain $D_c = K$, feedforward gain $D_r = K_r$, and global internal model matrices $(\mathbf{A}_I, \mathbf{B}_I)$ structured per Remark 2. The previous architectures are recovered through the canonical pairs (A_I, B_I) in Table 2:

- *Step tracking:* Setting $n_{x_I} = 1$ with $A_I = 0_{n_y \times n_y}$ and $B_I = I_{n_y}$ yields $x_I = \int_0^t e(\tau)\, d\tau \in \mathbb{R}^{n_y}$, recovering the multivariable PI tracking architecture of Santos et al. (2023) with $C_I = K_I \in \mathbb{R}^{n_u \times n_y}$.
- *Ramp and sinusoidal tracking:* For single-output systems ($n_y = 1$), setting $n_{x_I} = 2$ with (A_I, B_I) from Table 2 ($\alpha = 0$ for ramps, $\alpha = \omega^2$ for sinusoids) directly recovers the second-order

internal model structure of Santos et al. (2024) with $C_I = [K_{I_1} \; K_{I_2}]$.

Consequently, the methodology developed herein subsumes both static output-feedback tracking schemes (Santos et al. 2023, 2024) as particular cases, while establishing a unified synthesis framework that accommodates dynamic output-feedback compensation ($n_c \geq 1$), multi-channel outputs ($n_y > 1$), and all four canonical reference generators in Table 1.

3.1 Synthesis Optimization Program

The robust constrained control design problem is formulated as an optimization program over the polyhedral set parameter matrix L and the DOF controller gains. Specifically, we aim to construct a polyhedral RPI set

$$\mathcal{L} = \{\xi \in \mathbb{R}^{n_\xi} : L\xi \leq \mathbf{1}_l\}, \tag{15}$$

with $L \in \mathbb{R}^{l \times n_\xi}$, $\text{rank}(L) = n_\xi$, and $l > n_\xi$, which guarantees state and input constraint admissible trajectories under bounded reference signals $r \in \mathcal{R}$. Also, in this section, all the decision variables are defined in blue.

Lemma 1 *A polyhedron $\mathcal{L}$, (15), is a RPI set of the system (12), if and only if, there exists a Metzler matrix $H \in \mathbb{R}^{l \times l}$, a matrix $H_r > 0 \in \mathbb{R}^{l \times n_y}$ and a scalar $\gamma > 0$, such that*

$$\begin{aligned} HL &= L \begin{bmatrix} A + B(D_c - D_I)C & BC_c & BC_I \\ B_cC & A_c & 0_{n_c \times n_{x_I}} \\ -B_IC & 0_{n_{x_I} \times n_c} & A_I \end{bmatrix}, \\ H_rR &= L \begin{bmatrix} B(D_I + D_r) \\ 0 \\ B_I \end{bmatrix}, \\ H\mathbf{1}_l + H_r\rho &\leq -\gamma \mathbf{1}_l, \end{aligned} \tag{16}$$

where the matrices A_I and B_I are defined by the reference signal in Table 2. Furthermore, the closed-loop system matrix A_{cl} is Hurwitz, and its eigenvalues $\mu_i \in \sigma(A_{cl})$, for $i = 1, \ldots, n_\xi$, satisfy $\text{Re}(\mu_i) \leq -\gamma < 0$. Finally, the matrix L in (15) has complete column rank if and only if it admits a pseudo-inverse matrix $V \in \mathbb{R}^{n_\xi \times l}$ so that

$$VL = I_{n_\xi}. \tag{17}$$

Proof The existence of the Metzler matrix H ($H_{ij} \geq 0, \forall i \neq j$), the matrix $H_r > 0$, and the scalar $\gamma > 0$ verifying (16) is a necessary and sufficient condition for the RPI of the set $\mathcal{L}$ (Milani and Dórea 1996). Since for $\mathcal{L}$ we have assumed that $l > n_\xi$, the existence of V such that (17) holds is equivalent to $\text{rank}(L) = n_\xi$ (Brião et al. 2021). The first equality in (16) can be interpreted as a generalized similarity transformation that relates the spectral sets of A_{cl} and H, given by $\sigma(A_{cl}) = \{\mu_i, i = 1, \ldots, n_\xi\}$ and $\sigma(H) = \{\omega_j, j = 1, \ldots, l\}$, respectively. Thus, when $\text{rank}(L) = n_\xi < l$, we have $\sigma(A_{cl}) \subseteq \sigma(H)$. If $\gamma > 0$, the inequality in (16) implies that the Metzler matrix H is Hurwitz because the elements of its spectrum are such that $\text{Re}(\omega_i) \leq -\bar{\omega} \leq -\gamma$, where $-\bar{\omega}$ is necessarily a real eigenvalue belonging to $\sigma(H)$ (Castelan and Hennet 1993). Hence, we conclude that A_{cl} is also Hurwitz and satisfies $\text{Re}(\mu_i) \leq -\gamma$. □

To guarantee that the state and input constraints are admissible for the trajectories emanating from the RPI polyhedron $\mathcal{L}$, we consider the polyhedral set inclusions $\mathcal{L} \subseteq \mathcal{X}_{cl}$ and $\mathcal{L} \subseteq \mathcal{U}_{cl}$. The necessary and sufficient algebraic relations to obtain such inclusions can be obtained by applying an extension of Farkas' Lemma presented in Appendix A, as follows:

- There exists a non-negative matrix $T \in \mathbb{R}^{(l_x + 2n_{x_I}) \times l}$, satisfying

$$\begin{aligned} TL &= \begin{bmatrix} X & 0_{l_x \times n_c} & 0_{l_x \times n_{x_I}} \\ 0_{2n_{x_I} \times n_x} & 0_{2n_{x_I} \times n_c} & X_I \end{bmatrix}, \\ T\mathbf{1}_l &\leq \mathbf{1}_{l_x + 2n_{x_I}}. \end{aligned} \tag{18}$$

- There exist non-negative matrices $Q \in \mathbb{R}^{l_u \times l}$ and $Q_r \in \mathbb{R}^{l_u \times n_y}$, such that

$$\begin{aligned} QL &= U\left[(D_c - D_I)C \; C_c \; C_I\right], \\ Q_rR &= U(D_I + D_r), \\ Q\mathbf{1}_l + Q_r\rho &\leq \mathbf{1}_{l_u}. \end{aligned} \tag{19}$$

The primary result of this work is stated below.

Theorem 1 (Constrained Tracking Control Stabilization) *Consider the closed-loop system (12) under Assumption 1, the polyhedral sets (11), (13), and (14). Let (A_I, B_I) be the preassigned reference generator realization from Table 2 (or Remark 2), a given set complexity $l > n_\xi$ and a decay parameter $\gamma > 0$. If there exist solutions of*

$$\begin{aligned} \underset{\Gamma}{\textit{maximize}} \quad & \text{trace}(X_{I,1} + X_{I,2}), \\ \textit{subject to} \quad & (16) - (19), \end{aligned} \tag{20}$$

where

$$\Gamma = (H, H_r, T, Q, Q_r, A_c, B_c, C_c, D_c, C_I, D_I, D_r, L, V).$$

Then, the polyhedral set $\mathcal{L}$ is RPI, such that $\mathcal{L} \subseteq \mathcal{X}_{cl}$ and $K_\xi \mathcal{L} \oplus K_r \mathcal{R} \subseteq \mathcal{U}_{cl}$. Therefore, for any initial condition $\xi(0) \in \mathcal{L}$, the corresponding closed-loop trajectories satisfy the predefined constraints and the output y asymptotically tracks any reference trajectory $r \in \mathcal{R}$ generated by the reference dynamics in (5).

Proof The proof can be divided into two parts:

1) According to the Extended Farkas' Lemma (see Lemma 2 in the Appendix A), the existence of the non-negative matrix T satisfying the relation (18) provides necessary and sufficient conditions under which $\mathcal{L} \subseteq \mathcal{X}_{cl}$. Likewise, applying Lemma 2, the existence of non-negative matrices Q and Q_r verifying (19) or, equivalently,

$$\begin{aligned} \begin{bmatrix} Q & Q_r \end{bmatrix} \begin{bmatrix} L & 0 \\ 0 & R \end{bmatrix} &= U \begin{bmatrix} K_\xi & K_r \end{bmatrix}, \\ \begin{bmatrix} Q & Q_r \end{bmatrix} \begin{bmatrix} \mathbf{1}_l \\ \rho \end{bmatrix} &\leq \mathbf{1}_{l_u}, \end{aligned}$$

guarantees $K_\xi \mathcal{L} \oplus K_r \mathcal{R} \subseteq \mathcal{U}_{cl}$.

2) Under the conditions (16)-(17), for any reference signal $r \in \mathcal{R}$ and for all $\xi(0) = [x^T(0) \;\; x_c^T(0) \;\; x_I^T(0)]^T \in \mathcal{L}$, the closed-loop state trajectory remains inside $\mathcal{L}$ while fulfilling all the prescribed state and input constraints. Consequently, the system evolves in a domain where all the constraints are inactive, and the closed-loop dynamics are uniquely determined by the unconstrained linear model (12), whose state matrix A_{cl} is Hurwitz stable. Hence, the IMP is locally valid for any step, ramp, sinusoidal, or parabolic reference signal $r \in \mathcal{R}$ and for all $\xi(0) \in \mathcal{L}$, concluding the proof. □

Remark 4 Depending on the design requirements, the reference bound vector ρ in (11) can either be treated as predefined by operational limits or incorporated as a decision variable within the optimization program to maximize the allowable operational range (Santos et al. 2023). In the present framework, ρ is assumed to be a preassigned parameter, while the optimization focuses on synthesizing the controller gains, internal model limits, and the robust positively invariant set $\mathcal{L}$.

4 Numerical Simulation

In this section, the efficacy, constraint admissibility, and performance of the proposed dynamic output feedback synthesis are demonstrated through two benchmark systems. First, a single-input single-output (SISO) two-tank system subject to both state and actuator constraints is evaluated under piecewise-linear reference tracking and compared against an existing static output feedback method. Second, the pitch-axis longitudinal dynamics of an F-16 fighter aircraft are evaluated under harmonic reference tracking, covering both single-output and multi-input multi-output (MIMO) configurations in the presence of actuator saturation.

The synthesis program (20) is a non-convex nonlinear program (NLP) featuring bilinear matrix equality constraints arising from the Extended Farkas' Lemma and RPI set conditions. To solve this problem, we use the solver KNITRO (Byrd et al. 2006), which is well adapted to non-convex programs with algebraic equality constraints and has been validated in set invariance control synthesis (Brião et al. 2021; Santos et al. 2023; Ernesto et al. 2026). In particular, KNITRO implements an interior-point/conjugate-gradient (Interior/CG) algorithm combined with a multi-start heuristic that searches from multiple initial guesses across the parameter space, mitigating the risk of entrapment in undesirable local minima. To reduce the search space and improve numerical tractability, the decision variables were bounded as follows:

$$\begin{aligned} H_r, T, Q, Q_r \;\text{ in }\; &\left[0, 10^2\right], \\ A_c, B_c, C_c, D_c \;\text{ in }\; &\left[-50, 50\right], \\ H, L, C_I, D_I, D_r \;\text{ in }\; &\left[-10^2, 10^2\right], \\ V \;\text{ in }\; &\left[-10^3, 10^3\right]. \end{aligned}$$

4.1 Constrained Two-Tank System

Consider the linearized model of a two-tank system adapted from Ferramosca et al. (2011):

$$\begin{aligned} \dot{x} &= \begin{bmatrix} -0.0304 & 0.0187 \\ 0 & -0.0187 \end{bmatrix} x + \begin{bmatrix} 6.6667 \\ 10 \end{bmatrix} u, \\ y &= \begin{bmatrix} 1 & 0 \end{bmatrix} x, \end{aligned}$$

where the state and control inputs are subject to the bounds $-0.38 \leq x_1 \leq 0.68$, $-0.35 \leq x_2 \leq 0.65$, and $|u| \leq 2$.

To demonstrate the advantages of the proposed synthesis with dynamic compensation ($n_c = 1$), a comparative study is conducted against the PI-like framework ($n_c = 0$) reported in Santos et al. (2024), which is recovered as a special case in Remark 3. Both controllers are designed to track

the reference signal defined by:

$$r(t) = \begin{cases} 0.0025t, & 0 \le t \le 120\,\text{s}, \\ 0.3, & 120 < t \le 300\,\text{s}, \\ -0.0025t + 1.05, & 300 < t \le 500\,\text{s}, \\ -0.2, & t > 500\,\text{s}. \end{cases}$$

By solving the optimization program (20) with $l = 12$ facets, the ramp signal matrices A_I and B_I from Table 2, and allowable reference bounds $\rho = [0.3,\ 0.2]^\top$, the resulting controller parameters are:

$$\begin{aligned} A_c &= -0.0874, & D_c &= 2.6481, \\ B_c &= 49.9995, & D_I &= 3.9778, \\ C_c &= -7.6188 \times 10^{-6}, & D_r &= -2.8193, \\ C_I &= \begin{bmatrix} 0.1616 & 0.0042 \end{bmatrix}. \end{aligned}$$

The controller gains in Santos et al. (2024) are:

$$\begin{aligned} K &= -3.8881, \quad & K_{I_1} &= 0.3733, \\ K_r &= 3.3142, \quad & K_{I_2} &= 0.0085. \end{aligned}$$

The gains K and K_r correspond to the effective output feedback $(D_c - D_I)C$ and the composite feedforward gain $(D_I + D_r)$ in (9), while $C_I = \begin{bmatrix} K_{I_1} & K_{I_2} \end{bmatrix}$. Table 3 outlines the synthesis outcomes for both approaches.

The tracking performance and transient error response are depicted in Fig. 1. As shown in the upper plot, both controllers successfully achieve asymptotic offset-free tracking across all slope changes and steady-state regions without violating any physical state or actuator saturation constraints. However, the tracking error trajectories in the lower plot reveal key advantages of the proposed synthesis. During sharp trajectory corner transitions (e.g., at $t = 0, 120, 300$, and 500 s), the proposed DOF controller reduces the peak transient tracking error from 2.8×10^{-3} to 2.0×10^{-3}, representing an approximate 28% peak error reduction over Santos et al. (2024). Moreover, the extra degree of freedom provided by the dynamic controller state x_c yields superior dynamic damping and faster error decay.

Most notably, as reported in Table 3, projecting the RPI sets onto the common coordinates $(x, x_I) \in \mathbb{R}^4$ reveals that the proposed DOF synthesis increases the admissible 4D hypervolume from 1.0594 to 1.9720 (an 86% enlargement). This confirms that dynamic output feedback substantially enlarges the domain of attraction while guaranteeing constraint satisfaction.

4.2 Multivariable F-16 Fighter Aircraft

Consider the pitch-axis longitudinal dynamics of an F-16 aircraft adapted from Flores et al. (2009):

$$\begin{aligned} \dot{x} &= \begin{bmatrix} 0 & 1 & 0 \\ 0 & -0.87 & 43.22 \\ 0 & 0.99 & -1.34 \end{bmatrix} x + \begin{bmatrix} 0 & 0 \\ -17.25 & -1.58 \\ -0.17 & -0.25 \end{bmatrix} u, \\ y &= \begin{bmatrix} 1 & 0 & 0 \end{bmatrix} x, \end{aligned}$$

where x_1 represents the pitch angle (rad), x_2 is the pitch rate (rad/s), and x_3 denotes the angle of attack (rad). The control vector components are elevator deflection and flaperon deflection. The system is subject to symmetric actuator saturation $\|u(t)\|_\infty \le 60$, with unconstrained states.

The objective is to track the reference signal

$$r(t) = a \sin(\omega t),$$

with frequency $\omega = 0.05\,\text{rad/s}$ and amplitude $a = r_{\max} = 1.4855$, matching the maximum allowable value considered in Flores et al. (2009).

To ensure offset-free harmonic tracking, the internal model matrices A_I and B_I are configured according to Table 2 with $n_{x_I} = 2$. By selecting a dynamic controller order $n_c = 2$ and solving the non-convex synthesis problem (20) with $l = 16$ facets, the resulting controller matrices are:

$$\begin{aligned} A_c &= \begin{bmatrix} -50.0000 & 19.5766 \\ 17.2863 & -48.6894 \end{bmatrix}, \quad B_c = \begin{bmatrix} 50.0000 \\ -50.0000 \end{bmatrix}, \\ C_c &= \begin{bmatrix} -50.0000 & 50.0000 \\ -36.8995 & 50.0000 \end{bmatrix}, \quad D_c = \begin{bmatrix} 40.3394 \\ 34.0142 \end{bmatrix}, \\ C_I &= \begin{bmatrix} -22.8719 & 0.9259 \\ -1.3036 & -4.4165 \end{bmatrix}, \quad D_I = \begin{bmatrix} -47.2128 \\ -25.5840 \end{bmatrix}, \\ D_r &= \begin{bmatrix} 35.5966 \\ 25.5840 \end{bmatrix}. \end{aligned}$$

Table 3 Comparison with Santos et al. (2024)

Characteristic	Santos et al. (2024)	**Proposed**
Controller order n_c	0	1
Volume $\mathrm{Proj}_{(x,x_I)}(\mathcal{L})$	1.0594	1.9720
Peak tracking error $\|e\|_\infty$	2.8×10^{-3}	2.0×10^{-3}
Internal model parameters	$X_{I,1} = \mathrm{diag}(0.1000, 0.0487)$	$X_{I,1} = \mathrm{diag}(0.1000, 0.1000)$
	$X_{I,2} = \mathrm{diag}(0.1000, 0.0739)$	$X_{I,2} = \mathrm{diag}(0.1000, 0.0713)$
Closed-loop spectrum $\sigma(A_{cl})^\top$	$[-25.827, -0.059, -0.046, -0.037]$	$[-8.744, -0.093, -0.079, -0.046, -0.037]$

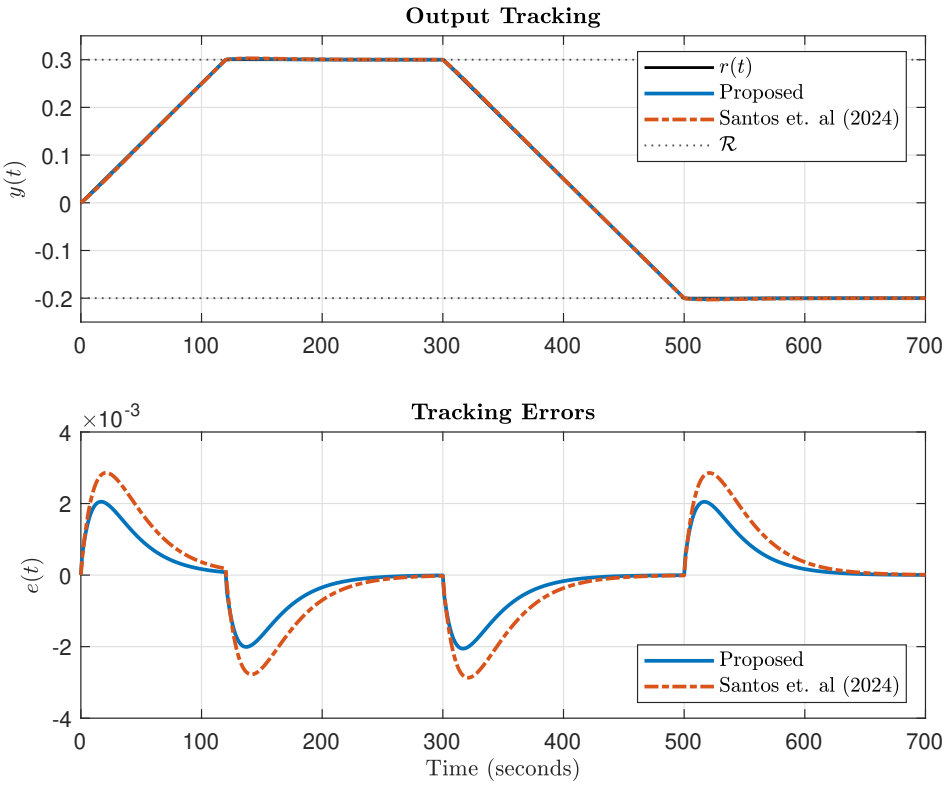


Fig. 1 Output tracking performance $y(t)$ and tracking error response $e(t)$ under the proposed controller (9) vs. Santos et al. (2024)

From X_I in (10), the resulting internal model bound vectors are:

$$X_{I,1} = \begin{bmatrix} 3.0284 & 0 \\ 0 & 10.0 \end{bmatrix}, \quad X_{I,2} = \begin{bmatrix} 3.2018 & 0 \\ 0 & 10.0 \end{bmatrix}.$$

The closed-loop matrix A_{cl} is Hurwitz with spectrum

$$\sigma(A_{cl}) = \{-28.2171 \pm 0.4159j,\ -23.5768,\ -16.3682,\ -2.8882,\ -1.5876,\ -0.0443\}.$$

The proposed framework is compared against the controller in Flores et al. (2009), parametrized by the state-feedback gain F and the anti-windup gain E_c:

$$F = \begin{bmatrix} 0.8480 & 1.2096 & 7.0338 & 0.0163 & 0.2789 \\ -1.9593 & 0.1896 & 2.7771 & -0.0333 & -0.5934 \end{bmatrix},$$

$$E_c = \begin{bmatrix} 3.2940 & 0.2136 \end{bmatrix}.$$

Both systems are simulated from the same initial conditions for the shared plant and internal model states, with $x(0) = [2.7359, -50.6254, 0]^\top$ and $x_I(0) = 0_{2\times 1}$. The dynamic controller state, present only in the proposed DOF synthesis, is initialized at $x_c(0) = [1.7130, -1.9341]^\top$.

The closed-loop tracking trajectories and control input profiles are illustrated in Fig. 2. As observed in the top plot, both controllers successfully eliminate steady-state tracking error due to the embedded harmonic internal model dynamics. However, the proposed architecture achieves significantly faster convergence, synchronizing with $r(t)$ in under 2 s and avoiding the underdamped oscillations of Flores et al. (2009), which requires roughly 20 s to settle.

In addition, both control channels strictly satisfy the actuator bounds $[-60, 60]$ across the complete time horizon. This comparison highlights an inherent control trade-off: whereas Flores et al. (2009) curtails the initial input action at the cost of a sluggish, oscillatory response that persists for 20 s, the proposed DOF design effectively utilizes the available actuator authority within the invariant set $\mathcal{L}$ to eliminate tracking lag in under one second, settling into the exact same steady-state control profile.

4.2.1 Extension to Multivariable Outputs

To demonstrate the scalability of the proposed framework to multi-input multi-output (MIMO) configurations ($n_u = 2, n_y = 2$), the F-16 longitudinal model is evaluated under the augmented measurement matrix

$$C = \begin{bmatrix} 1 & 0 & 0 \\ 0 & 0 & 1 \end{bmatrix},$$

where the pitch angle $x_1(t)$ and angle of attack $x_3(t)$ track harmonic references

$$r(t) = \begin{bmatrix} r_1(t) \\ r_2(t) \end{bmatrix} = \begin{bmatrix} a_1 \sin(\omega_1 t) \\ a_2 \sin(\omega_2 t) \end{bmatrix},$$

with $\omega_1 = 0.05$ rad/s, $\omega_2 = 0.03$ rad/s, and amplitude $a_1 = a_2 = 1.4855$.

To ensure tracking, independent harmonic internal models are embedded per Remark 2 ($n_{x_I} = n_y \cdot 2 = 4$):

$$\mathbf{A}_I = \begin{bmatrix} 0 & -\omega_1^2 & 0 & 0 \\ 1 & 0 & 0 & 0 \\ 0 & 0 & 0 & -\omega_2^2 \\ 0 & 0 & 1 & 0 \end{bmatrix}, \quad \mathbf{B}_I = \begin{bmatrix} 1 & 0 \\ 0 & 0 \\ 0 & 1 \\ 0 & 0 \end{bmatrix}.$$

Selecting dynamic controller order $n_c = 2$ and $l = 27$ facets, the optimization problem (20) is solved with the reference bounds fixed to the single-output benchmark amplitude $\rho = [1.4855, 1.4855]^\top$, resulting in the controller matrices:

$$A_c = \begin{bmatrix} -8.4696 & -1.0097 \\ -2.5883 & -9.9324 \end{bmatrix},$$
$$B_c = \begin{bmatrix} -0.8082 & 0.0123 \\ -2.5755 & 0.0414 \end{bmatrix},$$
$$C_c = \begin{bmatrix} 0.1512 & -0.5522 \\ 5.7662 & 20.2594 \end{bmatrix},$$
$$D_c = \begin{bmatrix} 12.6391 & 1.9172 \\ -4.6841 & -11.1617 \end{bmatrix},$$
$$D_I = \begin{bmatrix} 12.1384 & 1.9583 \\ -3.3470 & -41.1706 \end{bmatrix},$$
$$D_r = \begin{bmatrix} -12.1909 & -0.3721 \\ 3.4293 & 24.0204 \end{bmatrix},$$
$$C_I = \begin{bmatrix} -0.2636 & -0.0088 & 8.2695 & 6.5476 \\ 2.9998 & 0.1022 & -99.9978 & -81.0893 \end{bmatrix}.$$

From X_I in (10), the resulting allowable interval bounds for the internal model states are:

$$X_{I,1} = \mathrm{diag}(0.1160, 0.0100, 0.9796, 0.8198),$$
$$X_{I,2} = \mathrm{diag}(0.0749, 0.0104, 0.3668, 2.5767).$$

The closed-loop matrix A_{cl} is Hurwitz with spectrum

$$\sigma(A_{cl}) = \{-10.2777, -7.3545, -4.1072, -2.3548, -1.6706, -1.0641, -0.7167, -0.5181, -0.0435\}.$$

Figure 3 shows the closed-loop tracking response initialized from:

$$x(0) = [1.5926, -3.7086, -1.6528]^\top,$$
$$x_c(0) = [-0.1261, -0.5128]^\top,$$
$$x_I(0) = [-0.8057, -7.0154, -0.0314, -0.3791]^\top.$$

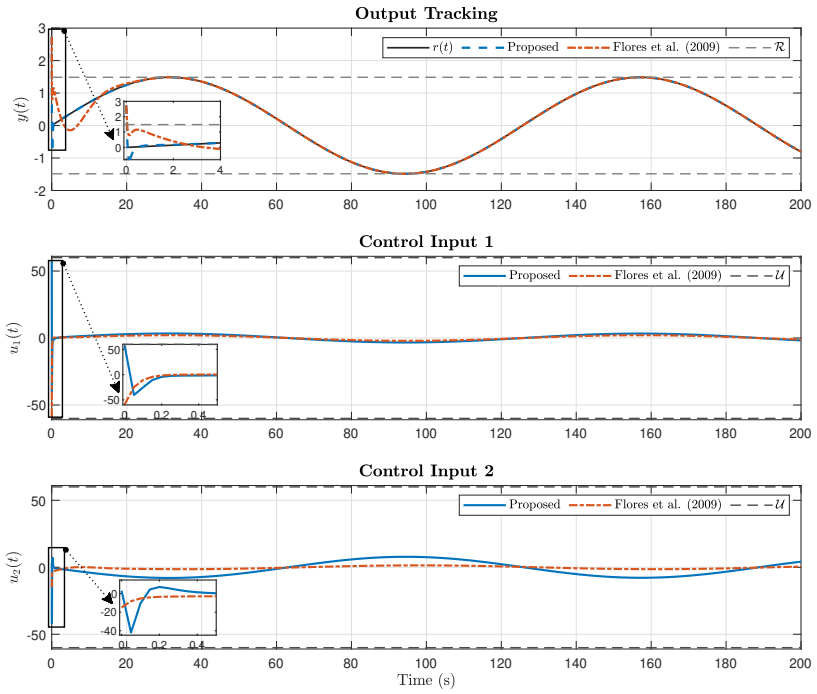


Fig. 2 Output tracking $y(t)$ and control inputs $u(t)$ under the proposed controller (9) vs. Flores et al. (2009)

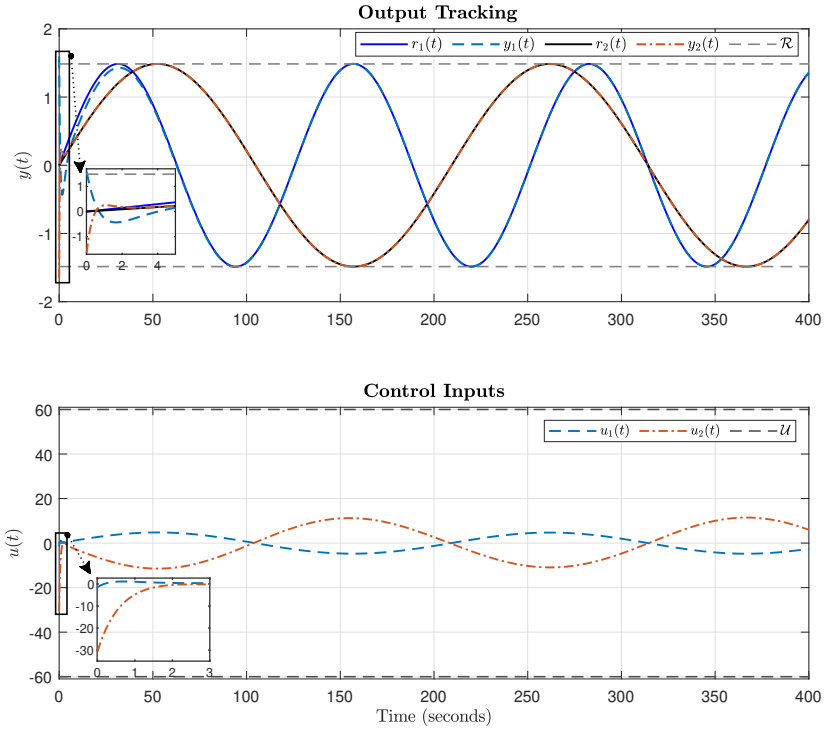


Fig. 3 Output tracking $y(t)$ and control inputs $u(t)$

Both outputs asymptotically track their independent harmonic reference signals with zero steady-state error, decoupling the longitudinal dynamics. The control inputs $u_1(t)$ and $u_2(t)$ remain strictly within the physical saturation limits $\|u(t)\|_\infty \leq 60$ during both transient and steady-state regimes, demonstrating the effectiveness of the proposed constrained output-feedback scheme in handling coupled multivariable dynamics.

Finally, it is worth noting that in both numerical examples, the dynamic controllers are designed with reduced orders ($n_c = 1$ for the two-tank system and $n_c = 2$ for the F-16 aircraft), highlighting the flexibility of the proposed optimization framework to synthesize dynamic output-feedback compensators of arbitrary user-defined order.

5 Conclusion

This paper presented a dynamic output feedback control synthesis framework for linear systems subject to persistent reference trajectories and polyhedral state and input constraints. By embedding a generalized internal model within an augmented dynamic output feedback architecture, the proposed method guarantees asymptotic, offset-free tracking across diverse exogenous signals, including steps, ramps, sinusoids, and parabolic profiles. Based on robust positive invariance theory and the Extended Farkas' Lemma, the dynamic controller gains, internal model bounds, and the robust positively invariant set are synthesized simultaneously through a single offline bilinear optimization problem.

Numerical evaluations demonstrated the effectiveness and scalability of the formulation. For a constrained two-tank system under piecewise-linear references, incorporating dynamic controller states reduced peak transient tracking errors by approximately 28% and enlarged the projected invariant set volume by 86% compared to a static output feedback baseline. Furthermore, evaluations on an F-16 longitudinal aircraft model illustrated fast harmonic convergence, multivariable tracking across independent output channels, and strict actuator saturation compliance during both transient and steady-state regimes. In addition, the numerical evaluations demonstrated the framework's capability to seamlessly synthesize reduced-order dynamic output-feedback controllers of arbitrary order tailored to the designer's complexity and performance requirements.

Acknowledgements. This work was supported in part by the Natural Sciences and Engineering Research Council of Canada (NSERC), and in part by CNPq-Brazil, Grants 308350/2026-0 and 406863/2023-7.

Appendix A Polyhedra and Invariance

This appendix recalls basic definitions for polyhedral sets and the Extended Farkas' Lemma adapted from Hennet (1995); Blanchini and Miani (2015).

Definition 1 *Any closed and convex polyhedral set $\mathcal{P}(\phi) \subseteq \mathbb{R}^n$ can be characterized by a shaping matrix $P \in \mathbb{R}^{l_p \times n}$ and a vector $\phi \in \mathbb{R}^{l_p}$, with l_p and n being positive integers, i.e.,*

$$\mathcal{P}(\phi) = \{x \in \mathbb{R}^n : Px \leq \phi\}. \tag{A1}$$

Note that $\mathcal{P}(\phi)$ in (A1) includes the origin as an interior point iff $\phi > 0$. In the sequel, if $\phi = \mathbf{1}_* = [1, 1, \ldots, 1]^T \in \mathbb{R}^*$, the resulting polyhedral set $\mathcal{P}(\mathbf{1}_*)$ will be denoted as $\mathcal{P}$.

Definition 2 *(Robust Positively Invariant Set) A polyhedral set $\mathcal{P}(\phi) \subseteq \mathbb{R}^n$ is said to be RPI for the system $\dot{x}(t) = f(x(t), d(t))$, $t \geq 0$, $x(t) \in \mathbb{R}^n$, $d(t) \in \Delta(\psi) \subseteq \mathbb{R}^{n_d}$, where $\Delta(\psi)$ is a compact polyhedral set, if for any initial state $x(0) \in \mathcal{P}(\phi)$, the state trajectory $x(t)$ remains bounded inside $\mathcal{P}(\phi), \forall\, t \geq 0$ and $\forall\, d(t) \in \Delta(\psi)$.*

Lemma 2 *(Extended Farkas' Lemma) Consider two polyhedral sets of $\mathbb{R}^n$ defined by $\mathcal{P}_i(\phi_i) = \{x \in \mathbb{R}^n, P_i x \leq \phi_i\}$, for $i = 1, 2$, with $P_i \in \mathbb{R}^{l_{p_i} \times n}$ and positive vectors $\phi_i \in \mathbb{R}^{l_{p_i}}$. Then, $\mathcal{P}_1 \subseteq \mathcal{P}_2$ if and only if there exists a non-negative matrix $Q \in \mathbb{R}^{l_{p_2} \times l_{p_1}}$ such that*

$$QP_1 = P_2,$$
$$Q\phi_1 \leq \phi_2.$$

References

Åström KJ, Hägglund T, Astrom KJ (2006) Advanced PID control, vol 461. ISA-The Instrumentation, Systems, and Automation Society Research Triangle Park

Blanchini F, Miani S (2015) Set-theoretic Methods in Control, 2nd edn. Birkhäuser

Brião SL, Castelan EB, Camponogara E, et al (2021) Output feedback design for discrete-time constrained systems subject to persistent disturbances via bilinear programming. Journal of the Franklin Institute 358(18):9741–9770

Byrd RH, Nocedal J, Waltz RA (2006) Knitro: An integrated package for nonlinear optimization. In: Di Pillo G, Roma M (eds) Large-Scale Nonlinear Optimization. Springer, Boston

Casavola A, Mosca E, Angeli D (2000) Robust command governors for constrained linear systems. IEEE Transactions on Automatic Control 45(11):2071–2077

Castelan EB, Hennet JC (1993) On invariant polyhedra of continuous-time linear systems. IEEE Transactions on Automatic control 38(11):1680–1685

Chen CT (2014) Linear System Theory and Design, 4th edn. Oxford University Press

Di Cairano S, Borrelli F (2015) Reference tracking with guaranteed error bound for constrained linear systems. IEEE Transactions on Automatic Control 61(8):2245–2250

Ernesto JG, Castelan EB, Lucia W (2026) Output feedback design for parameter varying systems subject to persistent disturbances and control rate constraints. International Journal of Robust and Nonlinear Control 36(7):4219–4233

Ferramosca A, Limon D, Alvarado I, et al (2011) Optimal MPC for tracking of constrained linear systems. International Journal of Systems Science 42(8):1265–1276

Figueiredo LS, Parreiras TAR, Lacerda MJ, et al (2020) Design of LPV-PI-like controller with guaranteed performance for discrete-time systems under saturating actuators. IFAC-PapersOnLine 53(2):3898–3903

Flores JV, da Silva Jr JMG, Sbarbaro D (2009) Robust periodic reference tracking for uncertain linear systems subject to control saturations. In: IEEE Conference on Decision and Control (CDC), IEEE, pp 7960–7965

Flores JV, da Silva JMG, Pereira LFA, et al (2011) Repetitive control design for MIMO systems with saturating actuators. IEEE Transactions on Automatic Control 57(1):192–198

Francis BA, Wonham WM (1976) The internal model principle of control theory. Automatica 12(5):457–465

Franklin GF, Powell JD, Emami-Naeini A (2010) Feedback Control of Dynamic Systems, 6th edn. Prentice Hall, Upper Saddle River, NJ

Garone E, Di Cairano S, Kolmanovsky I (2017) Reference and command governors for systems with constraints: A survey on theory and applications. Automatica 75:306–328

Gilbert EG, Ong CJ (2011) Constrained linear systems with hard constraints and disturbances: An extended command governor with large domain of attraction. Automatica 47(2):334–340

Hennet JC (1995) Discrete time constrained linear systems. Control and Dynamic Systems 71:157–214

Limon D, Alvarado I, Alamo T, et al (2005) MPC for tracking of piece-wise constant references for constrained linear systems. IFAC Proceedings Volumes 38(1):135–140

Milani BE, Dórea CE (1996) On invariant polyhedra of continuous-time systems subject to additive disturbances. Automatica 32(5):785–789

Santos GF, Castelan EB, Lucia W (2023) On the design of constrained PI-like output feedback tracking controllers via robust positive invariance and bilinear programming. IEEE Control

Systems Letters 7:1429–1434

Santos GF, Castelan EB, Lucia W (2024) A constrained tracking controller for ramp and sinusoidal reference signals using robust positive invariance. In: Proc. American Control Conference (ACC), Toronto, ON, Canada, pp 1670–1675

Tarbouriech S, Garcia G, da Silva JMG, et al (2011) Stability and Stabilization of Linear Systems with Saturating Actuators. Springer Science & Business Media